PHYSICAL REVIEW B **80**, 220104(R) (2009)

Atomistic simulation of the premelting of iron and aluminum: Implications for high-pressure melting-curve measurements

Sergey V. Starikov* and Vladimir V. Stegailov†
Joint Institute for High Temperatures, Russian Academy of Sciences, Moscow 125412, Russia
and Moscow Institute of Physics and Technology (State University), Dolgoprudny 141700, Russia
(Received 29 September 2009; revised manuscript received 3 December 2009; published 30 December 2009)

Using atomistic simulations we show the importance of the surface premelting phenomenon for the melting-curve measurements at high pressures. The model under consideration mimics the experimental conditions deployed for melting studies with diamond-anvil cells. The iron is considered in this work because of the long-standing discrepancies in its melting-curve measurements and its geophysical significance. Results for aluminum are presented for comparison as an opposite case. We calculate the premelting magnitude at different pressures and temperatures and show its influence on the surface roughness that can mislead the experimental determination of the onset of melting in diamond-anvil cells.

DOI: 10.1103/PhysRevB.80.220104 PACS number(s): 64.70.D−, 62.50.−p, 64.30.−t

The experimental determination of the iron melting curve at high pressure (more than 100 GPa) is a long-standing topic of interest. There is a considerable scatter in the experimental results obtained using the diamond-anvil cell (DAC) and shock-wave (SW) techniques.[1–17] The melting curves measured in DAC are located systematically at lower temperatures than it should be according to the results of SW measurements. The similar situation is observed for Ta, Mo, and W.[18,19] At the same time the experimental data on the melting curve of aluminum and some other metals do not contain this uncertainty.[11,20–23] Therefore any explanation of the contradictions in the experimental data for Fe should explain the absence of such contradictions for Al.

Many possible explanations were suggested but none of them is universally accepted. In SW experiments phase transitions are detected by the discontinuities in the longitudinal sound speed. During shock-wave loading, solids are heated inside as the shock front advances. The bulk melting starts at grain boundaries and defects of crystal structure.[24] Fast relaxation time allows equilibrium to be quickly established in shocked metals.[3,9] The probable superheating of a sample in SW measurements alone cannot explain the temperature discrepancies between shock and static measurements of melting of transition metals at $P>100$ GPa.[13] The hypothesis about new iron phase at high pressure was not confirmed by experiments.[10,16]

It is significant that the registration of melting in DAC experiments is based on the structural changes on the surface of a sample (such as motions of the laser speckle or changes in the position and intensity of the spots in the x-ray diffraction pattern). The exact nature of the changes observed at the onset of melting is not exactly clear.[12,16,25] In DAC experiments a sample is placed in a pressure medium (e.g., argon or Al_2O_3 or xenon). The presence of a pressure medium at the boundary of a solid sample can make the melting thermodynamics and mechanisms more complex that in a one component system. Note that the possible eutectic melting between iron and the argon pressure medium was not detected.[15]

In this work we make an attempt to illustrate the peculiarities of the melting mechanisms in DAC measurements deploying the atomistic simulation (AS) method. The AS results demonstrate that the surface melting of metal at the contact with disordered argon is accompanied by the premelting process. The premelting phenomenon consists in the formation of a thin, thermodynamically stable, liquidlike film at an interface for temperatures below the equilibrium melting temperature.[26–28] Due to premelting the surface layer obtains liquidlike properties and the surface gets the ability to be deformed. These facts may influence the reflectivity of the sample surface and may be the reason of motions of the laser speckle and changes in x-ray pattern in the DAC experiments. Thus the premelting may be an important peculiarity of the DAC experiments.

The AS method enables one to investigate phase transformations at the level of dynamics of individual atoms.[24,26–30] First the bulk melting is investigated in this work. The melting curves $T_m(P)$ of Fe and Al are obtained by the direct two-phase simulation method described in detail in Refs. 29 and 30. The simulation box has the dimensions 96 ± 2.5 Å in the x direction, 42 ± 1.5 Å in the y direction and 33 ± 1.5 Å in the z direction (during simulation the size of box changes for different pressures and temperatures). 17427 and 11610 atoms are used for Fe and Al, respectively. The interaction of metal atoms is described by embedded atom method (EAM) potentials proposed in Ref. 30 for h.c.p. and liquid phases of iron and in Ref. 31 for f.c.c. and liquid phases of aluminum.

We consider the pressures between 100 and 200 GPa for iron where the discrepancies in the melting-curve measurements are pronounced. For Fe in the this range of pressures the obtained dependence $T_m(P)$ agrees with the results of SW measurements[1,9] and matches the melting curve obtained in a similar way in Ref. 30 and is close to the recent *ab initio* results.[17] There is an essential distinction between the calculated dependence and the melting curves obtained in DAC experiments.[2,4,16] For the Al calculated melting curve (at lower pressures) agrees with DAC (Refs. 21 and 22) and SW experimental data[20] and theoretical calculations.[11,23]

The following stage of our research consists in two-component simulations. Atoms of Ar occupy one half of the simulation box. Atoms of metal (Fe or Al) are located in

TABLE I. The parameters of the exp-6 potentials.

Interaction	A (eV)	ρ (Å)	B (eV Å^6)
Ar-Ar[a]	3868	0.2962	62
Fe-Ar	4617	0.2752	70
Al-Ar	6810	0.2694	82

[a]Reference 33.

another half of the simulation box (the geometry is chosen to mimic the conditions of DAC measurements). One-half of the simulation box ($x>48$ Å) is filled with 8720 atoms of Fe (or 5860 atoms of Al) in the h.c.p. phase (or in the f.c.c. phase for Al), and the other half was filled 4450 atoms of argon in the disordered structure. Three dimensional periodic boundary conditions are used. There are two metal-argon boundaries in the simulation box. In order to simplify the model the layer of atoms that embraces one of the boundaries (5 Å in thickness) is frozen. The metal and argon atoms in this layer do not move in the course of simulation. The equilibrium parts of the AS trajectories obtained in the NVE ensemble are used for study premelting in this model. The corresponding values of pressure and temperature are averaged over the simulation box excluding two regions of phase boundaries and boundaries between components. Simulation box sizes are chosen in order to avoid the anisotropy of the pressure tensor at the accuracy of thermal fluctuations. All the calculations are carried out using the LAMMPS code.[32]

The argon-metal cross interaction is described by the exp-6 potential $U(r)=Ae^{-r/\rho}-B/r^6$. Parameters proposed in Ref. 33 are used for the Ar-Ar potential. The parameters of the metal-Ar potential are found by the following procedure. First for each metal the exp-6 potential is found that gives the best fit to the corresponding EAM-potential data on the equation of state and the melting curve in the range of temperatures and pressures considered. Then the mixing parameters for the metal-Ar interaction are approximated as $A_{ij}=\sqrt{A_{ii}A_{jj}}$, $\rho_{ij}=2(\rho_{ii}^{-1}+\rho_{jj}^{-1})^{-1}$, and $B_{ij}=\sqrt{B_{ii}B_{jj}}$, where i and j are the atom type (see Table I). These potentials provide immiscibility of argon and metals that agrees with the *ab initio* results.[15]

After the preparation of the system the phase transformation process starts spontaneously. In some temperature interval ΔT below the melting temperature T_m, the formation of a liquidlike layer of metal (Fig. 1) is observed between the disordered argon and the solid metal; i.e., there is a premelting. In order to trace the motion of the phase boundary we use the static structure factor η as an order parameter $\eta=\langle\cos(\mathbf{r}\cdot\mathbf{k})\rangle^2+\langle\sin(\mathbf{r}\cdot\mathbf{k})\rangle^2$, where $\mathbf{r}$ is an atom position, $\mathbf{k}$ is a reciprocal-lattice vector for the given crystal structure and the averaging $\langle\cdots\rangle$ is performed layer by layer along the x direction (the layers of 1–2 Å in thickness are parallel to yz plane). In the disordered phase η is close to zero. In the perfect lattice η equals to unity and becomes $\eta_{\max}\approx 0.5$ due to thermal fluctuations. Figure 1 shows an example of the η profile along with the profile of the relative concentration of Fe atoms $N_{\mathrm{Fe}}/N_{\mathrm{Fe+Ar}}$ (the data are averaged over 50 ps along the equilibrium AS trajectory). The thickness of disordered metal (Fe or Ar) layer L is calculated as $L=x_{[\eta=0.8\eta_{\max}]}-x_{[N_{\mathrm{Metal}}/N_{\mathrm{Metal+Ar}}=0.8]}$, where the first term is a condition for the phase boundary and the second term is a condition for the metal-Ar boundary.

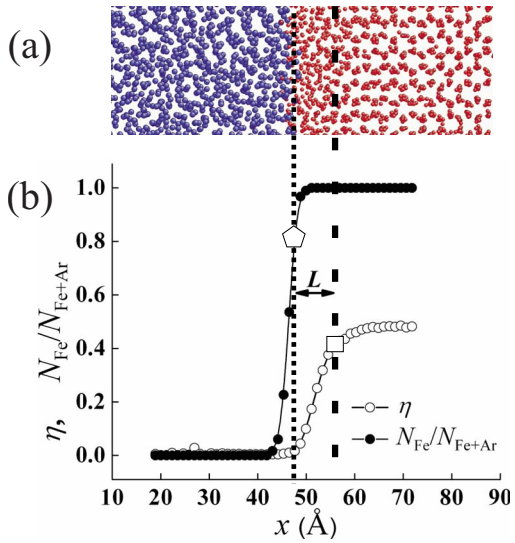

FIG. 1. (Color online) The arrangement of atoms in a two-component simulation projected to the xy plane (a): large blue atoms (left): disordered argon; small red atoms (right): h.c.p. iron. The respective distribution of the order parameter η and the relative concentration of iron $N_{\mathrm{Fe}}/N_{\mathrm{Fe+Ar}}$ along the x axis (b) are shown; a square shows $\eta=0.8\eta_{\max}$; a pentagon shows $N_{\mathrm{Fe}}/N_{\mathrm{Fe+Ar}}=0.8$; L is the thickness of the disordered iron layer.

Figure 2 shows the dependencies of the thickness of the disordered metal layer L on the difference T_m-T at fixed pressure P, where T_m is the melting temperature of metal calculated in the two-phase simulation and T is the temperature of the system. These results agree with the logarithmic dependence of the theory of surface melting[26] that gives

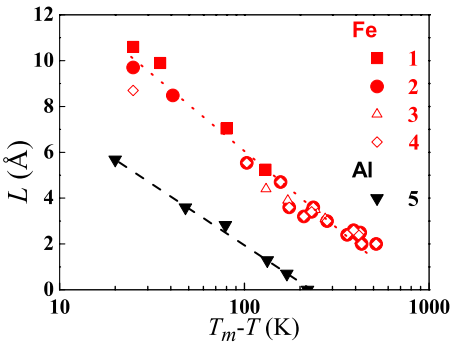

FIG. 2. (Color online) The dependence of the thickness of the disordered metal layer L (averaged over 50 ps along the AS trajectory) on the difference T_m-T. The results for Al and Fe are given. The pressures P and the surface orientations are 1: $P=149$ GPa $(10\bar{1}0)$; 2: $P=168$ GPa $(10\bar{1}0)$; 3: $P=185$ GPa $(11\bar{2}0)$; 4: $P=131$ GPa $(11\bar{2}0)$; and 5: $P=73$ GPa (100) (the last value is given for Al). The lines correspond to the best fits for ξ values according to Eq. (1).

TABLE II. Parameters of the metal-Ar system for Eq. (1).

Metal	P (GPa)	$\Delta\gamma$ (mJ/m^2)	T_m (K)	ρ_l (kg/m^3)	λ (MJ/kg)
Fe	168	300 ± 100	4450	11190	0.5 ± 0.05
Al	73	60 ± 20	3610	3630	1 ± 0.1

$$L = \xi \ln\left[\frac{T_m \Delta\gamma}{\xi \rho_L \lambda (T_m - T)}\right], \quad (1)$$

where ξ is a constant, $\Delta\gamma = \gamma_{s-\mathrm{Ar}} - (\gamma_{s-l} + \gamma_{l-\mathrm{Ar}})$ and $\gamma_{s-\mathrm{Ar}}$, γ_{s-l}, and $\gamma_{l-\mathrm{Ar}}$ are the surface energies for the interfaces between solid metal and liquid argon, solid and liquid metal and liquid metal and liquid argon, respectively, ρ_l is the liquid density and λ is the latent heat. We calculate all these parameters except ξ directly for the EAM based models of Fe-Ar and Al-Ar systems under consideration (see Table II). Then we determine that $\xi = 3.1 \pm 0.1$ Å and $\xi = 2.3 \pm 0.1$ Å give the best fits for Fe and for Al, respectively (see Fig. 2). There is no single parameter in the Eq. (1) that differs essentially for Fe and Al and thus could be responsible for the difference in L values. For aluminum the temperature interval of premelting ΔT ($\approx$100 K) is several times smaller than for iron ($\approx$500 K). No essential pressure dependence of ΔT and weak influence of the crystal surface orientation were found in this work.

The deformation of a metal surface is of a special interest since it most likely underlies the speckle motion in DAC measurements. A special 30 ns calculation is carried out in order to check the possibility of surface deformations caused by premelting. A model of a localized surface inhomogeneity of the size close to the value that can affect the optical reflectivity is considered. The simulation box has the dimensions 152 Å in the x direction, 206 Å in the y direction and 96 Å in the z direction with 184 000 atoms of Fe (in the h.c.p. structure) and 101 000 atoms of Ar (in the disordered structure). Initially one half of the box is filled with Fe atoms forming the inhomogeneity. The remaining space is filled with Ar atoms. The conditions of calculations are the following: pressure $P = 181$ GPa, temperature $T = 4510$ K ($T_m - T = 120$ K). Figure 3 shows the atomic structure at the initial state and after 30 ns. It is well visible that the surface inhomogeneity has smoothed out essentially. At premelting, a surface tension can make work on deformation of the surface. Quite probably that on the microsecond time scale the surface is capable to be deformed so seriously that the reflectivity of a sample changes. The duration of a typical single DAC measurement is much longer.[2,4,14]

Figure 4 summarizes the main results of our study. The calculated melting curves of iron and aluminum are shown together with the experimental data. For aluminum the melting curve obtained in this work is in an agreement with all the experimental results. On the contrary, the iron melting curve matches with the data of SW measurements only. The regions of premelting for Al and Fe obtained in the two-component simulations are shown. For aluminum the correction to the melting temperature caused by the premelting

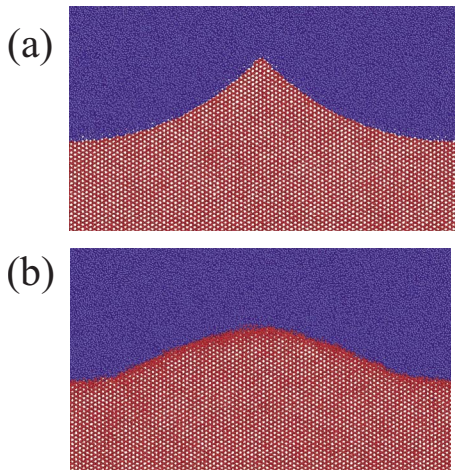

FIG. 3. (Color online) The simulation of the process of the surface inhomogeneity deformation (the xy plane projection): blue atoms (up): disordered argon; red atoms (below): h.c.p. iron. The initial structure (a) and the structure after 30 ns (b) are shown.

effect is not significant in comparison with experimental errors. But this effect is much more pronounced for iron. The premelting is observed up to ~500 K below the melting curve of h.c.p. iron at the range of pressure 100–200 GPa.

The presence of the local pressure anisotropy in the solid sample (that is very probable in DAC measurements) is capable to strengthen premelting effect appreciably.[26] Since the pressure anisotropy is deliberately avoided in this work we can consider the results obtained as the lower possible values of ΔT.

In this work we considered the atomistic model of the

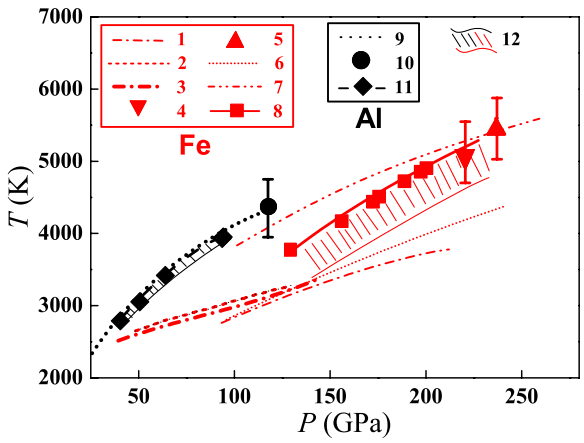

FIG. 4. (Color online) The comparison of the SW and DAC experimental melting curves for Fe and Al with the theoretical calculations of the melting curves and the premelting regions. The melting curves for Fe (DAC measurements): 1: Ref. 2; 2: Ref. 16; 3: Ref. 4. The melting points for Fe (SW measurements): 4: Ref. 1; 5: Ref. 9. The calculated melting curves for Fe: 6: Ref. 6; 7: Ref. 17; 8: Ref. 30; and this work. The data for Al: 9-melting line at DAC-measurements (Refs. 21 and 22) (results are shown by one curve); 10-melting point at SW-measurement (Ref. 20); 11-this work. The dashed regions (marked by 12) show the range of temperatures and pressures where the effect of premelting is observed in this work in the two-component metal-Ar system.

solid metal surface placed in contact with disordered argon. This setup models typical DAC experiments where the metal sample is immersed into the pressure medium. The EAM metal potentials deployed were shown to reproduce accurately the melting curve at high pressures in the direct two-phase simulations. We show that the presence of disordered argon at the surface leads to the premelting of the surface layer of metal. Its thickness was calculated for iron and aluminum at different pressures and temperatures and for different crystallographic orientations of the surface. Calculations showed that the premelting was essentially more pronounced for iron than for aluminum. The surface liquidlike layer is formed in iron several hundreds degrees below the melting temperature. The results are in a good agreement with the surface melting theory, however our calculations showed that it is no single parameter in Eq. (1) but their combination that leads to much stronger premelting of iron. Using the atomistic model of a localized surface inhomogenity we demonstrated that the premelting was able to remove surface roughness. Therefore the surface premelting can be one of the reasons for the underestimation of the melting temperature in the DAC experiments for iron and other substances that similarly exhibit strong premelting.

We are grateful to G. I. Kanel and I. V. Lomonosov for the useful discussions. Simulations were carried out on the computing cluster MIPT-60. The work was performed within the frameworks of the Program of Basic Research of the Presidium of the Russian Academy of Sciences (Program No. 12) and RFBR (Grants No. 09-08-01116 and No. 09-08-12161-ofi-m).

*starikov@ihed.ras.ru
†stegailov@ihed.ras.ru
‡http://www.ihed.ras.ru

[1] J. M. Brown and R. G. McQueen, J. Geophys. Res. **91**, 7485 (1986).
[2] R. Boehler, Nature (London) **363**, 534 (1993).
[3] C. S. Yoo, N. C. Holmes, M. Ross, D. J. Webb, and C. Pike, Phys. Rev. Lett. **70**, 3931 (1993).
[4] S. K. Saxena, G. Shen, and P. Lazor, Science **264**, 405 (1994).
[5] V. V. Brazhkin and A. G. Lyapin, Phys. Usp. **43**, 493 (2000).
[6] A. Laio, S. Bernard, G. L. Chiarotti, S. Scandolo, and E. Tosatti, Science **287**, 1027 (2000).
[7] T. J. Ahrens, K. G. Holland, and G. Q. Chen, Geophys. Res. Lett. **29**, 1150 (2002).
[8] A. I. Funtikov, High Temp. **41**, 850 (2003).
[9] J. H. Nguyen and N. C. Holmes, Nature (London) **427**, 339 (2004).
[10] Y. Ma, M. Somayazulu, G. Shen, H. K. Mao, J. Shu, and R. J. Hemley, Phys. Earth Planet. Inter. **143-144**, 455 (2004).
[11] D. Alfè, L. Vočadlo, G. D. Price, and M. Ross, J. Phys.: Condens. Matter **16**, S973 (2004).
[12] S. Japel, B. Schwager, R. Boehler, and M. Ross, Phys. Rev. Lett. **95**, 167801 (2005).
[13] S.-N. Luo and T. J. Ahrens, Phys. Earth Planet. Inter. **143-144**, 369 (2004).
[14] R. Boehler, EMU Notes in Mineralogy **7**, 273 (2005).
[15] S. Ostanin, D. Alfé, D. Dobson, L. Vočadlo, J. P. Brodholt, and G. D. Price, Geophys. Res. Lett. **33**, L06303 (2006).
[16] R. Boehler, D. Santamaria-Perez, D. Errandonea, and M. Mezouar, J. Phys.: Conf. Ser. **121**, 022018 (2008).
[17] D. Alfè, Phys. Rev. B **79**, 060101(R) (2009).
[18] D. Errandonea, Physica B **357**, 356 (2005).
[19] S.-N. Luo and D. C. Swift, Physica B **388**, 139 (2007).
[20] J. W. Shaner, J. M. Brown, and R. G. McQueen, in *Proceeding of High Pressure in Science and Technology*, edited by C. Homan, R. K. Mac Crone, and E. Whalley (North Holland, Amsterdam, 1984), pp. 137–141.
[21] R. Boehler and M. Ross, Earth Planet. Sci. Lett. **153**, 223 (1997).
[22] A. Hänström and P. Lazor, J. Alloys Compd. **305**, 209 (2000).
[23] I. V. Lomonosov, Laser Part. Beams **25**, 567 (2007).
[24] A. Yu. Kuksin, G. E. Norman, V. V. Stegailov, and A. V. Yanilkin, Comput. Phys. Commun. **177**, 34 (2007).
[25] M. Ross, R. Boehler, and D. Errandonea, Phys. Rev. B **76**, 184117 (2007).
[26] U. Tartaglino, T. Zykova-Timan, F. Ercolessi, and E. Tosatti, Phys. Rep. **411**, 291 (2005).
[27] S. V. Starikov and V. V. Stegailov, High Temp. **46**, 795 (2008).
[28] J. J. Hoyt, D. Olmsted, S. Jindal, M. Asta, and A. Karma, Phys. Rev. E **79**, 020601(R) (2009).
[29] J. R. Morris, C. Z. Wang, K. M. Ho, and C. T. Chan, Phys. Rev. B **49**, 3109 (1994).
[30] A. B. Belonoshko, R. Ahuja, and B. Johansson, Phys. Rev. Lett. **84**, 3638 (2000).
[31] X.-Y. Liu, Wei Xu, S. M. Foiles, and J. B. Adams, Appl. Phys. Lett. **72**, 1578 (1998).
[32] S. J. Plimpton, J. Comput. Phys. **117**, 1 (1995).
[33] M. Ross, J. Chem. Phys. **73**, 4445 (1980).